

CHAPTER IV

ELECTROPHORETIC DEPOSITION OF NANOPARTICLES OVER POLYMERS

Chapter Overview

The electrophoretic deposition (EPD) of colloidal nanoparticles like cadmium selenide (CdSe) onto conductive substrates like gold and silicon was well established in our laboratory and in the literature [41, 42]. Electrophoretically deposited films of these nanoparticles are characterized by low surface roughness and by homogeneous morphology on the micron scale. Because we targeted the fabrication of these films as free-standing objects, we needed a method to separate them from their original deposition substrates. We decided to investigate the idea of using a polymer as a sacrificial layer. In this scheme, nanoparticles would be deposited electrophoretically onto a polymer-coated substrate. The subsequent dissolution of the polymer would liberate the nanoparticle film from the substrate, yielding a free-standing films. The feasibility of this “sacrificial polymer layer” idea rested on the answer to the following question: *Do nanoparticle films—deposited by EPD atop a polymer layer—possess the same morphology as nanoparticle films deposited directly onto a conductive substrate?*

In this chapter, we report on the experiments to deposit CdSe nanoparticle films onto a dielectric polymer film (polystyrene). The CdSe films deposited over polystyrene were compared to CdSe films deposited on bare silicon. Scanning electron microscopy and atomic force microscopy showed that the CdSe films deposited atop polystyrene possessed morphology comparable to CdSe films deposited on the bare silicon electrodes, with both films exhibiting low surface roughness. We also review factors influencing the observed deposition, such as nanoparticle charging in suspension and wetting of electrode surfaces.

Having verified that high quality nanoparticle films can be deposited over a polymer layer, we performed depositions of iron oxide nanoparticles atop polystyrene and poly(lactic-co-glycolic acid). In this chapter, we report on the method of deposition for the iron oxide nanoparticles.

Further characterization of these nanoparticle films, which were central to the sacrificial layer investigation, is reserved for the next chapter.

4.1 Selection of Materials

CdSe nanoparticles dispersed in non-aqueous media, e.g. hexane, were an ideal colloidal system for this study because they can assume both positive and negative surface charges, which greatly facilitate the electric field-assisted deposition [24, 25]. While EPD of nanoparticles has traditionally been performed with conductive substrates, the evidence for sustained deposition of nanoparticles, even as the materials aggregate into a thick film, suggested the possibility of electrophoretically depositing nanoparticles directly onto a dielectric polymer layer. Our choice of polymer had to satisfy two physical criteria: (a) the breakdown electric field of the polymer must be larger than the applied electric field in our experiments; (b) swelling, dissolving, and electrochemical degradation of the polymer in the nanoparticle suspension, during EPD, must be minimized. Polystyrene was selected for its dielectric strength of 200 kV/cm [43], a threshold not exceeded in our electrophoretic deposition protocol, and its tolerance to hexane [44], the nanoparticle solvent that we employed during electrophoretic deposition.

4.2 Deposition of CdSe Nanoparticles on Polystyrene: Experimental Method

The CdSe nanoparticles were provided by Albert Dukes in the group of Professor Sandra Rosenthal. The method of Bowers, et al., [45] was modified to produce a single batch of monodisperse CdSe nanoparticles (core diameter ~ 4.5 nm) with dodecylphosphonic acid capping ligands (length ~ 2 nm). After synthesis, the nanoparticles were precipitated from the reaction mixture with methanol (Fisher Scientific). The particles' size and shape uniformity were verified by transmission electron microscopy (TEM) using a Philips CM-20 microscope.

For electrophoretic deposition, dilute suspensions of CdSe nanoparticles, of concentration $\sim 2.4 \times 10^{14}$ nanoparticles/ml, were prepared in high-purity hexane (Omnisolv, 99.97%). Nanoparticle suspensions were allowed to stabilize in darkness for 24 hours prior to

conducting the experiments. The concentration of the suspension was verified using nanoparticle extinction coefficient information [46] and absorbance measurements, recorded with a Varian Cary 5000 UV-VIS-NIR spectrophotometer. The hydrodynamic size and electrophoretic mobility of the nanoparticles were measured using a Malvern Instruments Zetasizer.

The electrophoretic deposition electrodes with dimensions 1 cm x 3 cm were prepared from n-type (Silicon Quest, resistivity 1-5 Ω -cm) and p-type (MEMC Electronic Materials, resistivity 0.005-0.025 Ω -cm) silicon wafers. The bare silicon electrodes were cut from the wafers, rinsed with ethanol (Pharmco) and de-ionized water, and dried with a stream of nitrogen. To prepare polystyrene-coated electrodes, the n-type silicon wafers were covered with a \sim 30 nm thick polystyrene film by spin coating. Films were cast from 4.4 mg/ml solutions of polystyrene (Polymer Source, $M_w = 212,000$, PDI = 1.05) in toluene (Fisher Scientific) by covering whole silicon wafers, previously rinsed with ethanol, with the solution and spinning for 60 s at 2,000 rpm. Subsequently, the wafers were baked at 90°C to aid solvent evaporation and polymer annealing. This temperature was used because the glass transition temperature of polystyrene in thin films (thickness < 150 nm) is lower than the bulk value of 102°C [47]. The polystyrene-coated electrodes were cut from the wafers, rinsed with de-ionized water, and dried with nitrogen. A small region of polystyrene was removed with acetone to enable a good electrical connection with the electrophoretic deposition circuitry.

A standard nanoparticle electrophoretic deposition setup was employed. Two vertically mounted, inward facing electrodes were separated by 2 mm in a parallel plate configuration. A bare n-type silicon (n-Si) electrode paired with a bare p-type silicon (p-Si) electrode served as the control set. To investigate the effects of depositing CdSe onto the polystyrene thin film, a polystyrene-coated n-type silicon (PS/n-Si) electrode was paired with a bare p-Si electrode. In all trials, the n-Si and PS/n-Si electrodes were biased negatively while the p-Si electrodes were biased positively. Before performing the nanoparticle deposition, I-V measurements in plain hexane over the range 0-250 V were used to determine the ohmic current for each electrode set. For deposition, the electrodes were submerged to approximately 1 cm depth in the nanoparticle suspension. We report on CdSe nanoparticle films deposited for 10 min using a constant applied

voltage of 250 V, supplied by a Keithley 6517A Electrometer/High-Resistance Meter. The Keithley Electrometer also recorded the electrophoretic currents. With hexane (dielectric constant ~ 1.9) between the electrodes, the effective electric field is ~ 660 V/cm. At the end of each electrophoretic deposition experiment, the electrodes were withdrawn from the liquid and kept at 250 V for an additional 5 min while the film dried. This step enables further densification of the deposit via local eddy currents [21].

The morphology and composition of electrodes and deposited films were characterized by scanning electron microscopy (SEM) and energy dispersive X-ray spectroscopy (EDS) using a Hitachi S-4200 microscope, operating at 5 kV and 10 kV, coupled to an EDS detector. The wetting of the electrode surfaces was assessed by measuring the advancing and receding contact angles of hexane using a Ramé-Hart manual contact angle goniometer, with assistance from Christopher Faulkner in the group of Professor Kane Jennings. Atomic force microscopy (AFM) was performed to assess surface topography of samples with a Digital Instruments Nanoscope III operating in tapping mode. AFM scans were analyzed using the NanoScope software. Polymer and nanoparticle film thicknesses were measured using a Veeco Dektak 150 profilometer.

4.3 Deposition of CdSe Nanoparticles on Polystyrene: Results and Discussion

This section presents data characterizing the nanoparticle size and electrophoretic mobility. The EPD current is presented. Characterization of the electrodes and the nanoparticle films is provided.

4.3.1 Electrode Characterization

Analysis of the n-Si and PS/n-Si electrodes prior to nanoparticle deposition (Figure 4-1) via AFM revealed smooth silicon and polystyrene deposition surfaces, both of which were characterized by a root-mean-square (RMS) roughness of 0.3 ± 0.1 nm. On the PS/n-Si electrodes, the polystyrene film coating was free of pinhole type defects. We used contact angle measurements of hexane to assess the extent to which the nanoparticle solvent wets the

electrode surfaces. The advancing contact angle was $\sim 14^\circ$ on the polystyrene-coated electrode and less than 10° on the bare silicon electrode. On both electrode types, the receding contact angle was less than 5° .

With such smooth electrode surfaces, any surface roughness or topology observed in the deposited nanoparticle films should be minimized and should be indicative of the nanoparticles and the deposition process itself. Theoretically, the 30 nm thick polystyrene film decreases the electric field between the electrodes by $\sim 0.01\%$. These substrate characteristics suggested that CdSe films deposited on the polystyrene-coated electrodes and on the bare electrodes would be of comparable quality and thickness. From the contact angle measurements, however, it is evident that the nanoparticle solvent, hexane, does not wet the polystyrene surface as readily as it wets the bare silicon surface. The lower affinity of hexane for polystyrene could have affected the “crossing over” of nanoparticles from the suspension phase to the solid phase at the electrode-suspension interface.

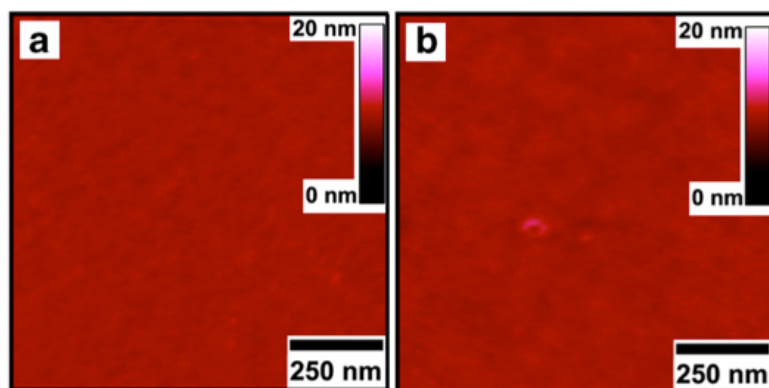


Figure 4-1. AFM images (a) of the bare silicon and (b) of the polystyrene-coated silicon electrodes prior to CdSe nanoparticle deposition.

4.3.2 Nanoparticle Deposition

Hexane suspensions of monodisperse CdSe nanoparticles with dodecylphosphonic acid capping ligands were prepared. The TEM image in Figure 4-2a confirms the nanoparticles' size and shape uniformity. We estimated the total diameter of a nanoparticle to be ~ 8.5 nm, from the

4.5 nm CdSe cores visible in TEM plus twice the ~ 2 nm ligand molecules that are not readily imaged in TEM. Figure 4-2b presents a size distribution of colloids in the nanoparticle suspension, collected via dynamic light scattering. A sharp peak centered at 7.5 nm attests the presence of single nanoparticles, within instrument error. The appearance of a second, broader peak centered at 23.5 nm suggests the presence of nanoparticle clusters, on average about three nanoparticles wide. Because CdSe nanoparticles have an electric dipole moment arising from asymmetric surface charge localization [48], charge-dipole and dipole-dipole interactions among the nanoparticles, in association with Coulomb interactions, may facilitate formation of a multi-nanoparticle cluster that remains stably suspended due to organic ligand capping. Clusters significantly wider than three nanoparticles are not observed, primarily because the nanoparticle concentration is relatively low—well below the 0.49 volume fraction that Shevchenko, et al., deemed necessary for entropy-driven solidification of a crystalline phase in solution [22]. Shevchenko et al., also arrived at this conclusion because Coulomb, charge-dipole, and dipole-dipole interactions drop off with increasing inter-nanoparticle distance [22].

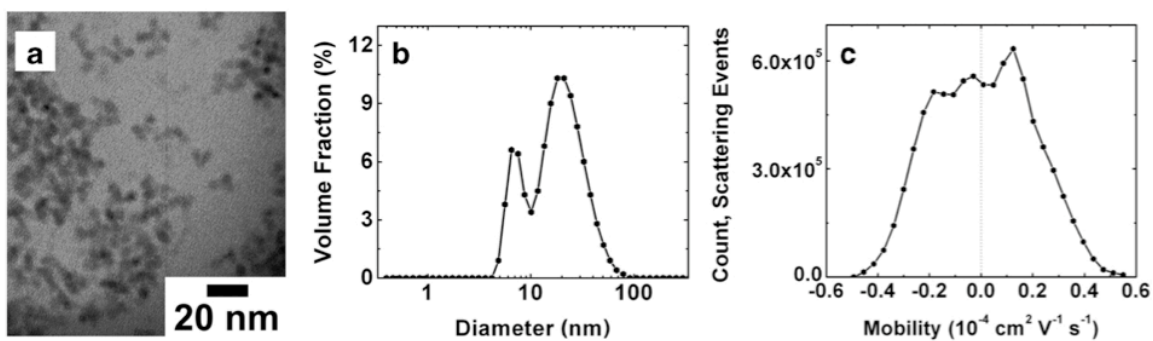


Figure 4-2. (a) TEM image of CdSe nanoparticles. (b) Size distribution of colloids in hexane suspension of CdSe nanoparticles. (c) Distribution of electrophoretic mobility of CdSe nanoparticles dispersed in hexane. The presence of both positively and negatively charged nanoparticles in the same suspension preparation is evident.

In all EPD trials, CdSe nanoparticles deposited on both the positively biased and negatively biased electrodes over the entire inward-facing area dipped in solution (approximately 1 cm x 1 cm), as is observed in previous nanoparticle EPD studies using nonpolar suspensions [41, 42]. We note that nanoparticles fail to deposit in a film covering the dipped area in the

absence of applied electric field. The origin of the charge state of the nanoparticles helps to explain why they deposit on both electrodes. After synthesis and precipitation, the CdSe nanoparticles can be dispersed stably in hexane. In such non-aqueous solvents, nanoparticle charging—both positive and negative—has been suggested to result from adsorption or desorption of ligand molecules at the nanoparticle surface [8], from thermal charging [25], and from ion exchange between nanoparticles and the suspension solvent [49].

The charge states present in a colloidal system may be probed by measuring the electrophoretic mobility of the constituent particles. Generally, the mobility μ gauges the velocity v of a particle in an applied electric field E [50].

$$\mu \equiv \frac{v}{E} = \frac{Ze}{3\pi\eta d} \quad (4.1)$$

μ may be calculated for a colloidal particle using the surface charge number Z , in units of elementary charge e , the solvent viscosity η , and the particle's hydrodynamic diameter d [51]. For suspensions measured using a constant electric field, the sign of the electrophoretic mobility corresponds to the sign of the particle's charge. The measurements by Shevchenko, et al., [23] reveal that an ensemble of surface charge states—positive, negative, and neutral—can be present in the same system of nanoparticles post-synthesis, depending on which ligand molecules are added to the nanoparticles. Data from Jia, et al., [24] show that the number of nanoparticle washing (precipitation) cycles, which directly relates to the quantity of ligand present in suspension, affects the mobility of nanoparticles and their corresponding charge states. We performed electrophoretic mobility measurements on our CdSe nanoparticles, which were precipitated from the reaction mixture and dispersed in hexane, then allowed to stabilize in darkness for 24 hours prior to measurement. Our results demonstrate the presence of nanoparticle populations carrying both positive and negative surface charge (Figure 4-2c) within the same suspension. The existence of CdSe nanoparticles exhibiting both charge states explains why nanoparticle films form on both electrodes during EPD.

Using $d = 8.5$ nm in equation (1), we calculate the CdSe nanoparticles have a mobility in hexane ($\eta = 0.326$ cP at 20°C) of $\mu = Z \times 0.61 \times 10^{-4} \text{ cm}^2 \text{ V}^{-1} \text{ s}^{-1}$. Figure 4-2c shows peaks in the distribution of mobility values at approximately $\pm 0.2 \times 10^{-4} \text{ cm}^2 \text{ V}^{-1} \text{ s}^{-1}$. If we assume that the nanoparticles have integer surface charge number $Z = \pm 1$, these peak locations imply that some colloidal constituents have hydrodynamic diameter approximately three times larger than that of a single nanoparticle, in agreement with the size distribution data of Figure 4-2b. The mobility peaks are relatively broad and appear at $\pm 0.2 \times 10^{-4} \text{ cm}^2 \text{ V}^{-1} \text{ s}^{-1}$ because recordings of light scattering, such as those occurring in laser Doppler velocimetry, are dominated by scattering events from the largest particles in a suspension. By all indications, the hexane suspensions of the nanoparticles are wholly stable; no flocculation or precipitation is observed. Thus, the particles deposited during EPD consist of individual nanoparticles and small agglomerates of nanoparticles.

The current measured in an EPD run is indicative of the motion and deposition of the charge-carrying nanoparticles themselves. Figure 4-3 presents current traces recorded during EPD with the (PS/n-Si, p-Si) and with the (n-Si, p-Si) electrode pairs, normalized by the deposition area on the electrodes. The two deposition traces (Figure 4-3c, d) have similar contours. An initial maximum current is followed by a continuous decline in the current as the accretion of nanoparticles onto the electrodes engenders a smaller voltage drop across the nanoparticle suspension and hence, a smaller electric field in the suspension. Current densities on the order of 1 nA/cm^2 to 10 nA/cm^2 are reasonable and expected, as the electrolytic contribution to the EPD current is minimal in a purified hexane suspension of nanoparticles. The EPD current for the (PS/n-Si, p-Si) electrode pair is nearly 10 times greater than that for the (n-Si, p-Si) electrode pair, an unexpected result since we would expect the presence of a polymer to slightly attenuate the current, not increase it. Prior to the EPD runs, we verified the dielectric nature of the polystyrene film by recording currents with each set of electrodes in plain hexane while applying the deposition voltage of 250 V. The current readings using either set of electrodes in hexane were fractional picoamperes larger than the open-circuit current measured in air, 174.5 pA. The measured current density in hexane for the (n-Si, p-Si) control set of

electrodes is 351 pA/cm^2 . When using the (PS/n-Si, p-Si) electrode pair in hexane, the measured current density is lower, 279 pA/cm^2 . This attenuation of current when using the polystyrene-coated electrode is reasonable, given that AFM showed the polystyrene to be well packed and free of defects.

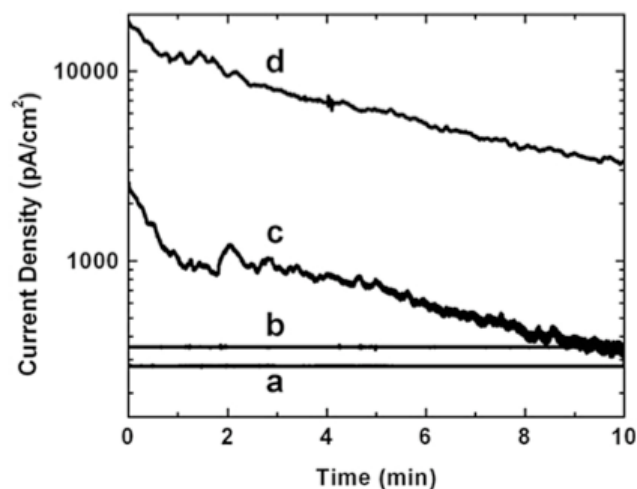


Figure 4-3. Current density measured in plain hexane at 250 V using (a) the PS/n-Si electrode and (b) the n-Si electrode, each paired with a p-Si electrode. Current density measured during nanoparticle EPD using (c) the n-Si electrode and (d) the PS/n-Si electrode, each paired with a p-Si electrode.

Hypothetically, if there were defects in the polystyrene layer, we would anticipate the EPD current density for the (PS/n-Si, p-Si) electrode pair to approximately equal, not to surpass, the EPD current density for the (n-Si, p-Si) electrode pair. It is possible that the elevated electrophoretic current when using the (PS/n-Si, p-Si) pair arises from molecular level interactions of the polystyrene film with the ligands on the CdSe nanoparticles. The styrene monomers that constitute the polymer each possess an aromatic phenyl group. With their delocalized π -electron system, aromatic groups may function as electron donors, without necessarily forming a covalent bond to the electron-accepting entity [52, 53]. Because nanoparticle charge is presumed to be localized to surface sites and mediated by ligand attachment, interactions of these ligands with the polystyrene aromatic groups at the electrode-nanoparticle interface may enhance the rate of charge transfer between the nanoparticles and the electrode, giving rise to the elevated current

measurement. Further investigation will be necessary to pinpoint the cause of the elevated electrophoretic current when using the polystyrene-coated electrode.

4.3.3 Nanoparticle Film Characterization

Films of CdSe nanoparticles can be prepared over a thin dielectric polymer layer using EPD. The microscale morphology of the CdSe films deposited on polystyrene is comparable to the microscale morphology of the CdSe films deposited on bare silicon (Figure 4-4). Both films, indicated as region IV, appear homogeneous at the millimeter length scale. There is a minor difference between the two samples: the band-like features at the top edge of the CdSe films, indicated as region III, appear wider in the PS/n-Si sample than in the n-Si sample. The CdSe nanoparticles deposited at the top edge have this band morphology because the evaporation of solvent during EPD leaves behind nanoparticles on the electrode as the solvent level decreases. The wider bands in the PS/n-Si sample, suggesting more rapid withdrawal away of the solvent from the substrate, may be attributed to hexane's lower affinity for polystyrene. Nonetheless, EDS confirmed the deposition of CdSe nanoparticles on both the PS/n-Si and n-Si electrodes. Figure 4-5 shows representative spectra for the polystyrene-coated electrodes pre (b) and post (a) CdSe nanoparticle deposition.

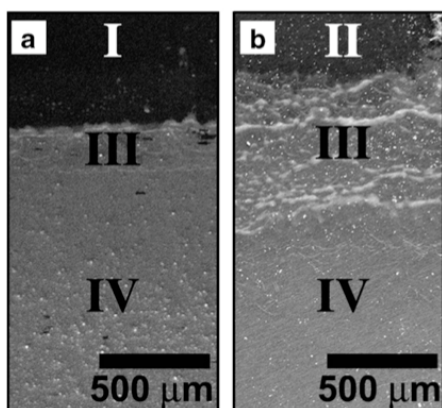


Figure 4-4. SEM images of CdSe nanoparticle film deposited (a) on the n-Si electrode and (b) on the PS/n-Si electrode. The features indicated are I, silicon; II, polystyrene; III, CdSe film edge due to solvent meniscus; IV, CdSe film. The band-like features of region III result from solvent evaporation, and are wider in (b) than in (a) due to hexane's poor affinity for polystyrene.

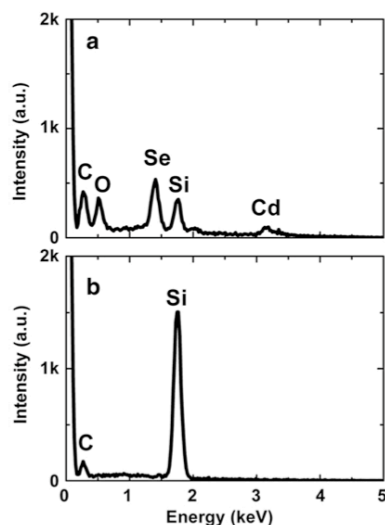


Figure 4-5. EDS spectra of (a) CdSe nanoparticle film deposited over polystyrene, corresponding to region IV in Figure 4-4b, and (b) an unused polystyrene-coated silicon electrode. The cadmium and selenium peaks affirm the presence of CdSe nanoparticles atop the polymer film. The oxygen signal in (a) originates from the dodecylphosphonic acid ligands capping the nanoparticles.

The thickness of the CdSe films was measured using a profilometer. Variations in the thickness of an individual film were attributed to electric field gradients near the electrode edges due to deviations from the parallel electrode configuration. CdSe films that were deposited on the PS/n-Si electrodes were thinner than those deposited on the n-Si electrodes, 420 ± 15 nm versus 1158 ± 26 nm. This discrepancy may be attributed to the lesser wetting of polystyrene by hexane, as determined from our contact angle measurements. In contrast, CdSe films deposited on the corresponding bare p-Si electrodes exhibit nearly equal thickness, 365 ± 12 nm on p-Si paired with PS/n-Si electrodes and 355 ± 13 nm on p-Si paired with n-Si electrodes. This similarity in thickness reflects the preparation of nanoparticle suspensions with a consistent population of negatively charged nanoparticles. Because both the n-Si and PS/n-Si electrodes have thicker CdSe films than their corresponding p-Si electrodes, it may be concluded that the nanoparticle suspension preparation yields a slightly greater population of positively charged nanoparticles. The mobility distribution of Figure 4-2c corroborates this conclusion.

A detailed probe of surface morphology with AFM reveals that the nanoparticles are tightly packed in arbitrary arrangements in both films (Figure 4-6). The smooth appearance of the

films in the SEM images is corroborated by RMS roughness values much lower than the diameter of one nanoparticle. Over a $1\ \mu\text{m} \times 1\ \mu\text{m}$ scanned area, the RMS roughness measured via AFM of CdSe films on the n-Si electrode is $2.7 \pm 0.1\ \text{nm}$, while CdSe films on the PS/n-Si electrode are nominally rougher, $2.8 \pm 0.1\ \text{nm}$. At this length scale, the films cannot be differentiated from each other. Thus, the incorporation of a thin dielectric polymer on a substrate does not affect the morphology of the nanoparticle films being electrophoretically deposited onto the polymer.

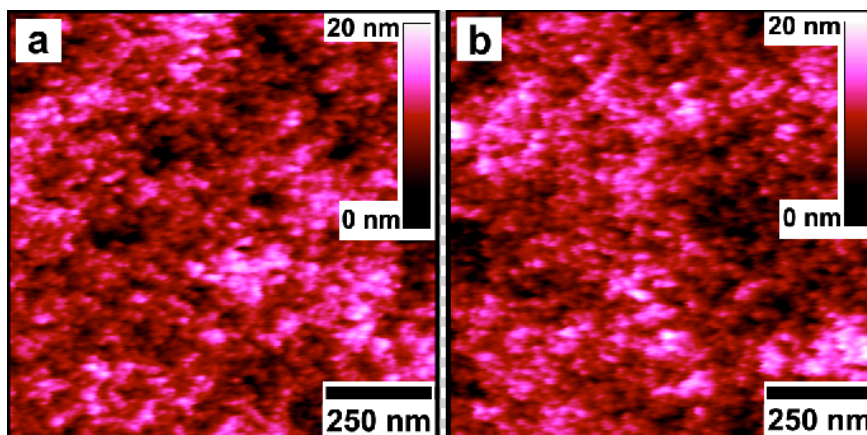


Figure 4-6. AFM images of CdSe nanoparticle films deposited (a) on the n-Si and (b) on the PS/n-Si electrodes.

4.4 Deposition of Iron Oxide Nanoparticles on PLGA

Having confirmed from the CdSe-polystyrene experiments that nanoparticles can be deposited in tightly packed films with microscale homogeneity atop a polymer layer, we sought to apply the technique to a wider selection of materials. As we detail in the next chapter, two different compositions of polymer were tested for the sacrificial layer process to produce free-standing nanoparticle films. The bulk of the sacrificial layer experiments were performed using iron oxide nanoparticles synthesized in our laboratory. In this section, we detail the preparation of substrates coated with poly(lactic-co-glycolic acid) (PLGA), the synthesis of iron oxide nanoparticles and their deposition onto the polymer-coated substrates.

4.4.1 Preparation of PLGA-coated Substrates

On Si wafers (as-delivered), we evaporated ~ 20 nm Cr adhesion layer and ~ 125 nm Au. These thicknesses were verified by ellipsometry, using a J.A. Woolam M-2000 Spectroscopic Ellipsometer and the materials' optical properties provided in the instrument's software. The PLGA polymer ($M_w = 9,700$, Sigma-Aldrich) was dissolved in chloroform at a concentration of 15 mg/ml, and spun cast on the Au surface at 2,000 rpm for 60 s. This procedure yielded PLGA layers with thickness 75 ± 2 nm, as measured by ellipsometry using the parameters described in [54]. The PLGA thickness was verified with profilometer measurement as well.

4.4.2 Synthesis of Iron Oxide Nanoparticles

Iron oxide nanoparticles were synthesized using the method of Park et al [55]. Iron oleate precursor was formed by reacting 2.16 g $\text{FeCl}_3 \cdot 6 \text{H}_2\text{O}$ (Sigma Aldrich, 98% Reagent Grade) with 7.33 g sodium oleate (TCI) in a solvent comprising 12 ml deionized water, 16 ml ethanol, and 28 ml hexane at 70 °C for 4.5 h. The upper layer containing iron oleate was rinsed with deionized water several times and removed using a separatory funnel. Iron oleate was heated further at 75°C for 24 h under vacuum. NPs were then grown by decomposition of 1.36 mmol iron oleate with 0.8 mmol oleic acid in 10 ml 1-octadecene. The mixture was heated to 320 °C at a rate of 3.3 °C/min and allowed to reflux for 40 minutes, then cooled to room temperature. As shown in Figure 4-7, this preparation yields iron oxide NPs with total diameter ~ 17 nm (core diameter 14 nm, oleic acid ligands total ~ 3 nm).

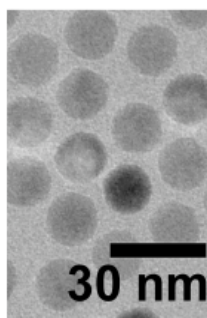


Figure 4-7. TEM image of iron oxide nanoparticles with oleic acid ligands, synthesized from iron oleate precursor.

We prepared the EPD suspension by removing the nanoparticles from 1-octadecene and suspending them in hexane. First, we combined 1 ml of the synthesis product with 5 ml hexane and 15 ml acetone, and then centrifuged the resulting mixture for 45 min at 3500 rpm. The nanoparticles, immiscible with acetone, precipitated out of the suspension during the centrifugation. After pouring out the supernatant, the nanoparticles were suspended in hexane at a concentration of $\sim 2.5 \times 10^{13} \text{ ml}^{-1}$ to perform EPD. The electrophoretic mobility measurement of the iron oxide nanoparticles in hexane is shown in Figure 4-8. These nanoparticles, too, exhibited both positive and negative charges. The mobility value for charges $Z = -1$ and $Z = +1$, calculated using Equation (4.1), are indicated in the figure.

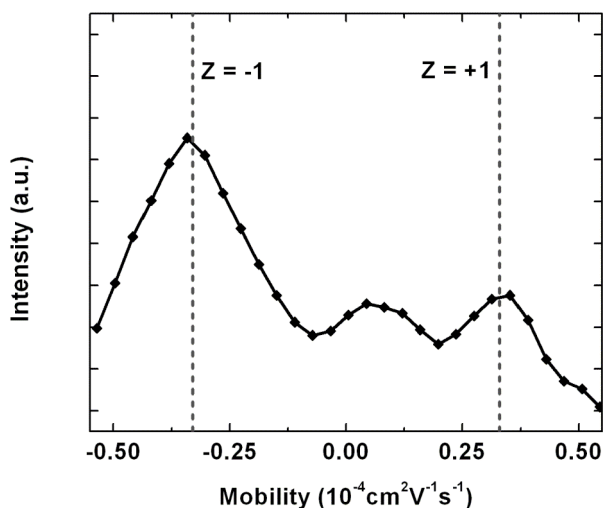


Figure 4-8. Electrophoretic mobility distribution of iron oxide nanoparticles in hexane.

4.4.3 EPD of Iron Oxide Nanoparticle Films

The EPD of iron oxide nanoparticles was performed in the above-described hexane suspension using two inward-facing parallel electrodes spaced 2 mm. The electrodes were roughly 1.5 cm x 3 cm in dimension. We deposited the iron oxide nanoparticle films using 600 V

applied dc voltage for 25 minutes. Here we used a longer time and a higher voltage compared to those used in the CdSe experiments (25 min vs. 10 min, 600 V vs. 250 V) because the iron oxide nanoparticles were suspended at $\sim 10\times$ lower concentration than the CdSe nanoparticles. A representative plot of the EPD current for iron oxide nanoparticles is shown in Figure 4-9. Like the current for deposition of CdSe nanoparticles, the current is on the order of nanoamperes. This is reflective of the low electrolytic current that arises when depositing nanoparticles from high-purity hexane.

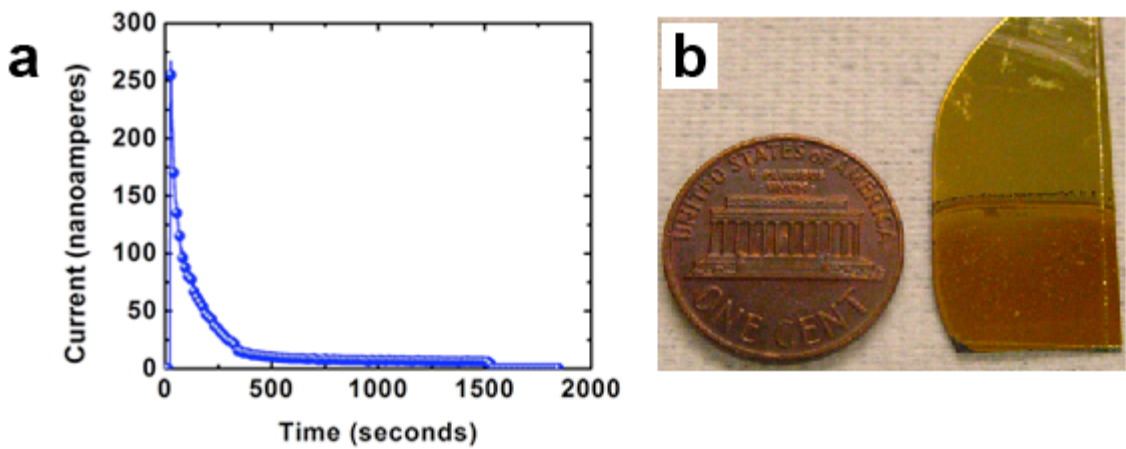


Figure 4-9. (a) Current for 25 min EPD of iron oxide nanoparticles, followed by 5 min drying with the voltage still applied. (b) Photograph of iron oxide nanoparticle film deposited on PLGA-coated Au electrode.

The iron oxide nanoparticles were driven to the electrode's surface, where they aggregated to form a solid film with homogeneity on the centimeter scale (Figure 4-9). Profilometry showed that the films possessed thicknesses ranging from 300 to 400 nm. These films, which were deposited on electrodes coated with polystyrene and with PLGA, were the focus of the sacrificial layer experiments attempting to produce free-standing nanoparticle films. The sacrificial layer study is reported in the next chapter.